

A simplified model of airway narrowing due to bronchial mucosal folding

Graham M. Donovan*, Merryyn H. Tawhai

Auckland Bioengineering Institute, University of Auckland, Private Bag 92019, Auckland Mail Centre, Auckland 1142, New Zealand

ARTICLE INFO

Article history:
Accepted 22 February 2010

Keywords:
Mucosal folding
Airway resistance
Bronchoconstriction
Basement membrane
Mathematical modelling

ABSTRACT

Bronchial mucosal folding during bronchoconstriction can be a significant phenomenon, and a number of previous studies have provided models which examine a number of aspects of this important problem. Previous approaches include finite-element analyses, fluid–structure interaction, linear elasticity models, geometrical computer optimisation, and more. These models have focused on changes to the elastic properties of the airways due to mucosal folding, rather than airway narrowing, and suffer from too great a degree of computational complexity for use in multiscale, spatially distributed models of the lung now being developed. We propose a simplified, geometrical model of airway folding under the assumptions of fixed airway wall area, fixed basement membrane perimeter during constriction, specified shape and number of folds, and liquid filling of the mucosal folds, in the context of determining effective airway radius and hence airway impedance. We show that this model generates predictions in good agreement with existing models while being vastly simpler to solve.

© 2010 Elsevier B.V. All rights reserved.

1. Introduction

The bronchial airways may develop mucosal folding during bronchoconstriction, wherein rather than contracting in a radially uniform manner, the airway develops a number of folds (Carroll et al., 2000; Lambert et al., 1994; Okazawa et al., 1995; Seow et al., 2000). The problem is akin to the buckling of a cylinder under pressure, where the number of folds developed is determined by the buckling mode. Bronchial mucosal folding has been thought physiologically important for two principal reasons: first, that it influences the mechanical and elastic properties of the airway; and second, that the folding affects the resistance to airflow through the airway. A number of studies have examined potentially important aspects of airway folding using several different approaches including fluid–structure interaction (Heil, 1999; Heil and White, 2002; Heil et al., 2008), finite-element (FEM) analyses (Wiggs et al., 1997), linear elasticity models which result in boundary value problems (Flaherty et al., 1972; Lambert et al., 1994), geometrical computer optimisation (Seow et al., 2000), mechanotransduction and the importance of compressive stresses (Tschumperlin et al., 2004; Tschumperlin and Drazen, 2006), and other approaches (cf. Kamm, 1999).

While these previous approaches have many advantages, they suffer from being quite difficult to solve in practice, especially for more than a single airway. The need for a simplified model of

folding is exemplified by the development of multiscale, spatially distributed models of the lung which potentially require computing a folding solution for each airway at any given time. The model we propose attempts only to determine how the airflow is affected by the folded, constricted airway, rather than considering the changes to the elastic airway properties due to folding. Under the assumption of liquid filling of the folded regions (Heil, 1999; Yager et al., 1989), this amounts to finding an effective luminal radius for a given degree of airway constriction. That is, this model depends on a separate model of the mechanical airway properties to determine the uniform airway radius, for example that of Lambert et al. (1982). The existing methods in the literature are difficult to adapt to these requirements. The fluid–structure and FEM approaches are computationally too costly. The linear elasticity approach involves solving a boundary value problem for a third or fourth order ordinary differential equation which always admits the unfolded, uniform, trivial solution. Ensuring that a numerical solver always finds the non-trivial folded solution is again a difficult problem. The geometrical computer optimisation approach likewise suffers from a need to conduct an exhaustive numerical search of all possible folding shapes. This is not tractable for a multiscale, spatially distributed model that aims to compute bronchoconstriction through a large number of airways. Several important studies include airflow as a critical factor in predictions of behaviour for bronchoconstricted asthmatic airways (Anafi and Wilson, 2001; Venegas et al., 2005) but do not account for folding; the inclusion of a folding model may improve the predictions of these models.

Moreover, the elastic mechanical properties of the peripheral airways in particular are not well understood, and models thereof often depend on extrapolation from central airway data as well

* Corresponding author. Tel.: +64 9 373 7599x85360; fax: +64 9 367 7157.
E-mail address: g.donovan@auckland.ac.nz (G.M. Donovan).

Nomenclature

r_0	outer radius of airway wall
Δr_0	initial thickness of airway wall
δr_0	amount of contraction of outer airway wall
r, θ	polar coordinates
$f(\theta)$	assumed functional form of folded boundary
P	original basement membrane perimeter
P'	constricted basement membrane perimeter
A	original airway wall area
A'	constricted airway wall area
N	number of folds
δN	change in number of folds N
r_u	radius of uniformly contracted airway (no folding)
r_{eff}	effective luminal radius of folded airway

Greek letters

α, β	parameters describing folded boundary
γ	expression used for compactness—see Section 2.2

as calibration with airflow data (cf. Lambert et al., 1982). An easily applied model of mucosal folding might help to quantify the potential impact of the phenomenon on these models.

We propose that a geometrical model, developed under assumptions used elsewhere in the literature, can be used as an effective alternative to the existing, more complex models. Complete details of the model are presented in the next section. We then demonstrate the effectiveness of this model in comparison with one existing approach, the collapsible tube model (Flaherty et al., 1972; Lambert and Wilson, 1972; Lambert et al., 1994) and find that the model predictions are in good agreement while being vastly easier to solve.

2. Model

To develop the simplified geometrical model, we employ two basic assumptions, as in Seow et al. (2000): first, that the material of the airway wall is incompressible, and second, that the area of the basement membrane is constant under constriction. If the airway is dilated, the wall is still considered incompressible but the basement membrane is allowed to stretch (McParland et al., 2004; Noble et al., 2005). In the plane, the area of the airway wall is constant, and the perimeter of the basement membrane is constant during constriction.

Rather than attempting to solve for all possible folded shapes, we make several assumptions. First, that the number of folds for a given airway order is known physiologically *a priori*. Second, we assume that the folding pattern is symmetric with the number of folds. The validity of these assumptions, and alternatives, as well as the method of determination of the number of folds are addressed in Section 4. We then assume a functional form of the folded basement membrane, described by two parameters. Then for a given degree of constriction, finding the folded solution amounts to solving a system of two equations (airway wall area and basement membrane perimeter, each held constant) with two unknowns (the two parameters).

We take the initial unconstricted outer radius of the airway to be r_0 and the initial thickness of the airway wall to be Δr_0 . The airway is then constricted by an amount δr_0 so that the outer (circular) boundary of the airway wall has constricted radius $(r_0 - \delta r_0)$. See Fig. 1 for an illustration of this configuration. The folded inner boundary has N folds and hence N -fold rotational symmetry, so that in general the folded boundary is given in polar coordinates where θ is the radial angle from 0 to $2\pi/N$ and α and β are the two

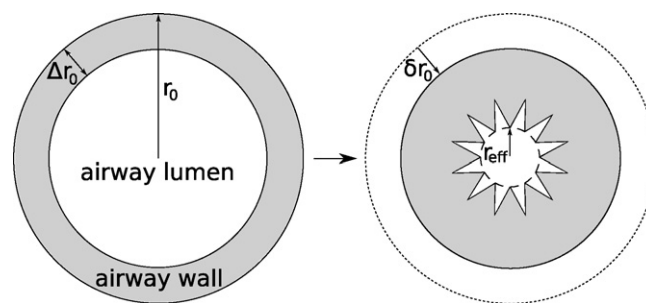


Fig. 1. Diagram of the folding airway wall model. When unconstricted (and undilated) the airway wall has outer radius r_0 and thickness Δr_0 . When the outer radius is constricted by an amount δr_0 (i.e. to $r = r_0 - \delta r_0$) the inner boundary of the airway folds such that the airway wall area and basement membrane perimeter are both preserved. Under the assumption of liquid filling of the folds, the effective luminal radius r_{eff} is determined by the point on each fold nearest to the centre of the lumen.

parameters determining the folded boundary. The interpretation of the parameters α and β depends on the assumed form of $f(\theta)$, which will be discussed in the following sections. We use the notation $r = f(\theta; \alpha, \beta)$ to indicate that the radius of the folded boundary depends on the independent variable θ (the polar coordinate angle) as well as parametrically on α and β . This partial folded boundary is then extended periodically another $(N - 1)$ times around the airway to generate the complete folded boundary. This 2D model does not account for axial variation along the airway.

The constraints are then as follows. The initial airway wall area is given by $A = \pi(r_0^2 - (r_0 - \Delta r_0)^2)$ and the folded airway wall area is computed by the integral

$$A' = \underbrace{\pi(r_0 - \delta r_0)^2}_{\text{wall and lumen area}} - \underbrace{\frac{N}{2} \int_0^{2\pi/N} f^2(\theta; \alpha, \beta) d\theta}_{\text{folded lumen area}}. \quad (1)$$

Here the two terms correspond to the areas of the entire constricted airway and the folded airway lumen, respectively. The initial basement membrane perimeter is $P = 2\pi(r_0 - \Delta r_0)$ and the perimeter of the folded boundary is obtained by integrating the arc length (cf. Lynch and Ostberg, 1970) as

$$P' = N \int_0^{2\pi/N} \sqrt{f^2(\theta; \alpha, \beta) + \left(\frac{d}{d\theta}f(\theta; \alpha, \beta)\right)^2} d\theta. \quad (2)$$

Then the two constraints $A = A'$ and $P = P'$ are used to determine the two parameters, α and β . The model is purely geometrical and intended to account for airway narrowing in a straightforward fashion; the modified mechanical properties of the airway due to folding are not addressed. In particular, the strain energy associated with these configurations is not addressed. This model approximates the implied radius rather than the strain energy.

2.1. Sigmoidal folding

We consider and compare two types of assumed folded boundaries, a sigmoidal folding pattern and a linear folding pattern. The sigmoidal boundary is given by

$$r = f(\theta; \alpha, \beta) = \beta - \alpha \sin(N\theta) \quad (3)$$

so that α controls the amplitude of the folds and β the average radius of the folded boundary. With this assumed form, Eq. (1) can be evaluated as

$$A' = \pi(r_0 - \delta r_0)^2 - \pi \left(\frac{\alpha^2}{2} + \beta^2 \right). \quad (4)$$

Unfortunately, with this assumed form, Eq. (2) cannot be usefully evaluated analytically. However, the integral can be evaluated

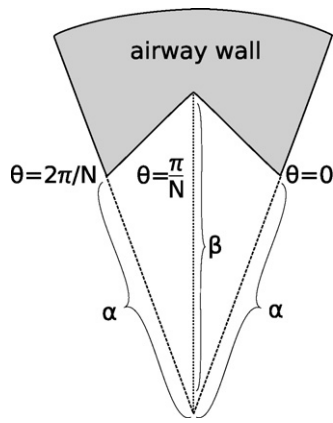


Fig. 2. Diagram of one segment of the linear folding model. With N folds, a single segment spans the angle $\theta = 0 \dots 2\pi/N$. The folded boundary consists of two line segments, connecting the points of radius α at $\theta = 0$ and $\theta = 2\pi/N$ with the point with radius β at $\theta = \pi/N$.

numerically or via Jacobi elliptic functions and a simple optimisation problem for α and β can be solved using standard MATLAB functions. See Appendix A for details.

2.2. Linear folding

The second folding form we consider is the linear, straight-line approximation. On each folded segment, for θ from 0 to $2\pi/N$, the folds connect the points with radius α at angles $\theta = 0$ and $\theta = 2\pi/N$ with the point with radius β at $\theta = \pi/N$. See Fig. 2 for a schematic of this arrangement.

With this simple arrangement the folded airway wall area and basement membrane perimeters can be constructed geometrically and are given by

$$A' = \pi(r_0 - \delta r_0)^2 - \alpha\beta N \sin\left(\frac{\pi}{N}\right) \quad (5)$$

$$P' = 2N\sqrt{\alpha^2 - 2\alpha\beta \cos\left(\frac{\pi}{N}\right) + \beta^2}. \quad (6)$$

Imposing $A' = A$ and $P' = P$ and solving, one obtains expressions for the parameters

$$\alpha^2 = \frac{1}{2} \left\{ \left(2\gamma \cos\left(\frac{\pi}{N}\right) + \frac{P^2}{4N^2} \right) \pm \sqrt{\left(2\gamma \cos\left(\frac{\pi}{N}\right) + \frac{P^2}{4N^2} \right)^2 - 4\gamma^2} \right\} \quad (7)$$

$$\beta = \frac{\gamma}{\alpha} \quad (8)$$

where we take $\gamma = [\pi(r_0 - \delta r_0)^2 - A]/[N \sin(\pi/N)]$ for compactness. In some situations this approximation may be inappropriate, principally either when α (and hence β) is complex, or when the folds bulge outside the airway wall ($\max(\alpha, \beta) > r_0 - \delta r_0$). In the former case we assume that the basement membrane perimeter contracts, but that the airway wall area is preserved exactly. Thus we take the uniform circle solution with radius

$$r_u = \sqrt{(r_0 - \delta r_0)^2 + \Delta r_0^2 - 2r_0\Delta r_0} \quad (9)$$

in the case where either α or β is imaginary. The conditions for complex-valued parameters can easily be found but unfortunately are not instructive. In the latter case, we likewise enforce the isoarea

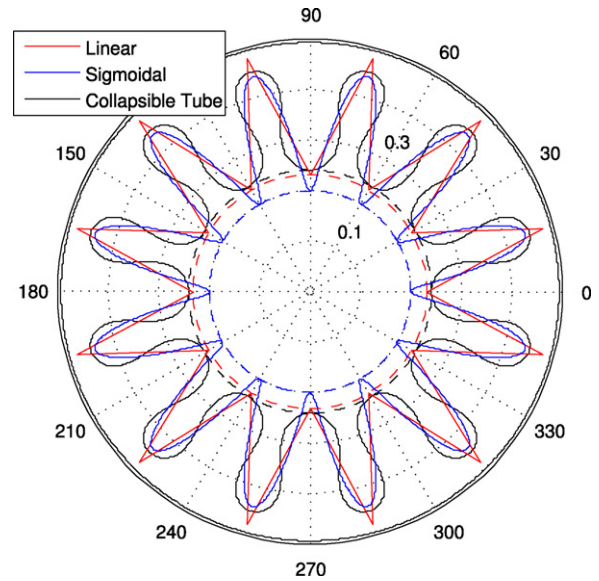


Fig. 3. Folding model comparison. Three folded boundaries given for the same degree of airway constriction in an airway of Horsfield order 1. The solid curves represent the folded boundary for each of the models. The dashed circles represent the corresponding effective luminal radii.

constraint but relax isoperimeter, and take the folded solution $\alpha = r_0 - \delta r_0$, with $\beta = \gamma/\alpha$ from the constraint $A' = A$.

An example of the folded inner airway boundaries computed with both of these models is given in comparison with that found by the collapsible tube model of Lambert et al. (1994) in Fig. 3. The collapsible tube model is given in black, the sigmoidal model in blue, and the linear model in red. The circles of corresponding effective radius are given by the dashed curves.

The effective luminal radius for each folded boundary is the largest uniform circle which fits inside the folded airway. This is the effective radius under the assumption of liquid filling of the folded areas. For the sigmoidal case, this minimal radius is given by $r_{\text{eff}} = \beta - |\alpha|$ and in the linear case by $r_{\text{eff}} = \min(\alpha, \beta)$, where both parameters are non-negative.

Of course, one might assume a functional form different from the two that we have considered. With a different assumed form, one would need to repeat the calculations we have performed for the sigmoidal and linear cases. The sigmoidal form was taken as a physically realistic shape for the folded airway, while the linear case is a simpler-still approximation for which there is a closed-form solution. Other assumed forms were tested, but none were found to perform better than those presented here (data not shown).

3. Model performance

To assess the performance of the simplified model, we compute effective airway radii with each model and compare with the results obtained with the model in Lambert et al. (1994). We repeat this calculation for each airway Horsfield order in the human lung (Horsfield et al., 1982), and across the entire range of constriction for that airway. The airway dimension parameters are taken from Lambert et al. (1982), and the assumed number of folds for each order is fit to and extrapolated from data in Carroll et al. (2000); Okazawa et al. (1995). The full parameter set used for this study appears in Table 1. We have opted to use a parameter for a fixed number of folds for a given airway order, rather than calculating the lowest-energy buckling mode (Lambert et al., 1994; Wiggs et al., 1997). Such buckling mode calculations can differ significantly from the physiologically observed folding numbers, and several theories have been advanced to explain this discrepancy

Table 1

Model parameters. Airway dimension parameters taken from Lambert et al. (1982), and the assumed number of folds for each order as fitted and extrapolated from data in Carroll et al. (2000); Okazawa et al. (1995) at zero pressure. We have then taken the radius r_0 to be the radius at a transmural pressure of 490 Pa using the model of Lambert et al. (1982) to approximate functional residual capacity. Airways are classified according to Horsfield order (Horsfield et al., 1982).

Horsfield order	r_0 (mm)	Δr_0 (mm)	No. of folds N
1	0.263	0.017	12
2	0.281	0.017	13
3	0.298	0.017	13
4	0.316	0.018	14
5	0.338	0.018	14
6	0.366	0.018	15
7	0.391	0.019	16
8	0.427	0.019	16
9	0.473	0.020	17
10	0.533	0.022	18
11	0.608	0.023	18
12	0.695	0.025	19
13	0.802	0.027	19
14	0.923	0.029	20
15	1.054	0.032	20
16	1.207	0.036	20
17	1.397	0.039	20
18	1.620	0.044	20
19	1.872	0.049	20
20	2.197	0.056	20
21	2.588	0.063	20
22	2.994	0.071	20
23	3.452	0.078	20
24	3.993	0.088	20
25	4.660	0.099	21
26	5.645	0.110	21
27	6.968	0.127	21
28	8.514	0.159	21

(Carroll et al., 2000; Lambert, 1991; Lambert et al., 1994; Seow et al., 2000). We have taken the radius below which folding occurs (r_0) to be the radius at a transmural pressure of 490 Pa using the model of (Lambert et al., 1982) to approximate functional residual capacity.

First we assess the degree of difference between the effective luminal radius calculated with each model and that which is obtained by assuming uniform constriction. The results of these

calculations are shown in Fig. 4 for several representative airway orders. All three models predict significant reduction in effective radius versus uniform constriction. However, the sigmoidal model tends to overestimate this effect relative to the collapsible tube model, and the linear model gives the best agreement.

Principally the airway radius is of interest in calculating airway impedance. Using our model results for effective airway radius, and under the assumption of Poiseuille flow, we calculate the airway resistance (the real part of impedance) in each of these representative airway orders for a given degree of constriction. The resistance values are normalised such that the resistance of the unconstricted airway is 1. The results of this calculation are given in Fig. 5. The dashed curve indicates the resistance under uniform constriction. All three models predict significant increases in airway resistance, as expected given the predicted decrease in effective radius. Again the sigmoidal model tends to overestimate the airway resistance relative to the collapsible tube model, and the linear model gives the best agreement. Note that as resistance is given on a log scale, the difference between the uniform and folded models is very significant, especially for the smaller airways. For the Horsfield Order 1 airway in Fig. 5, for example, at $\delta r_0/r_0 = 0.2$ the uniform and linear predictions of resistance differ by more than 50%.

To demonstrate the cumulative effect of folding on airway tree resistance, we use a simple model of a conducting airway tree containing 90 asymmetric-branching airways, ranging from Horsfield order 1–10. We compute the baseline resistance of this airway tree at functional residual capacity using radius values from Table 1, using the method of Lutchen and Gillis (1997). We then constrict the outer radius of each airway by 20% and compute r_{eff} under both uniform constriction and linear folding and again calculate the resistance. The results of these calculations are given in Fig. 6, which shows a marked increase in airway resistance under folding versus uniform constriction.

The simple linear model appears to provide good agreement with the more sophisticated collapsible tube model for the purpose of computing effective radius and thus resistance at the sampled airway orders. To assess the performance of the linear model for all airways, we calculate the relative error in radius prediction between the linear model and the collapsible tube model

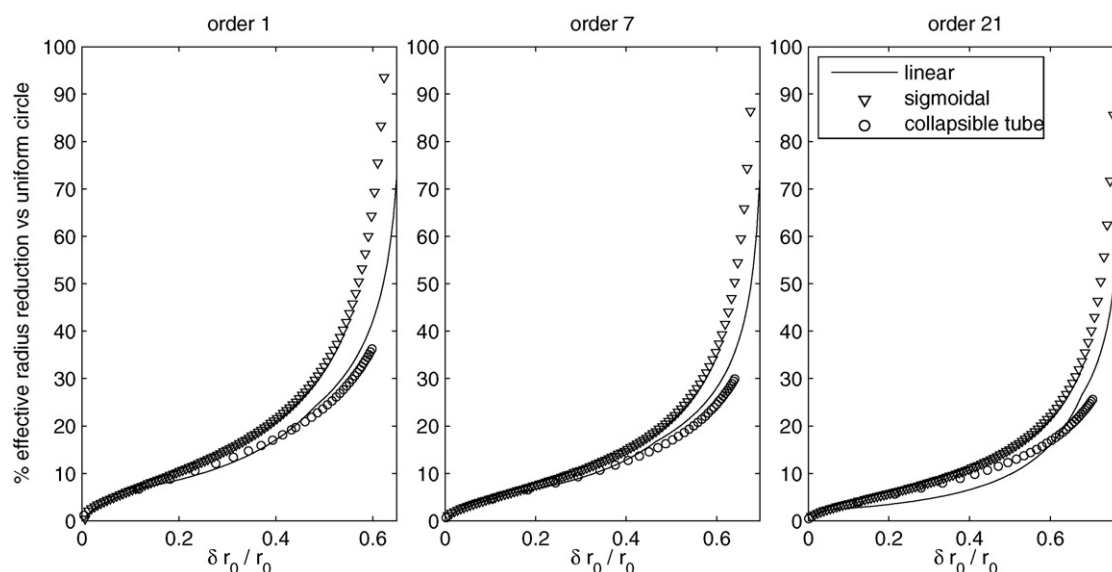


Fig. 4. Airway radius reduction due to folding. Reductions in effective airway radius compared with uniform constriction as predicted by each folding model for selected airway Horsfield orders, as a function of normalised constriction. Each folding model predicts a significant decrease in effective luminal radius versus uniform constriction. The collapsible tube model is solved for increasing constriction up to the point of contact between adjacent folds. The linear model provides the best agreement with the collapsible tube model. Order 1 corresponds to the terminal bronchiole.

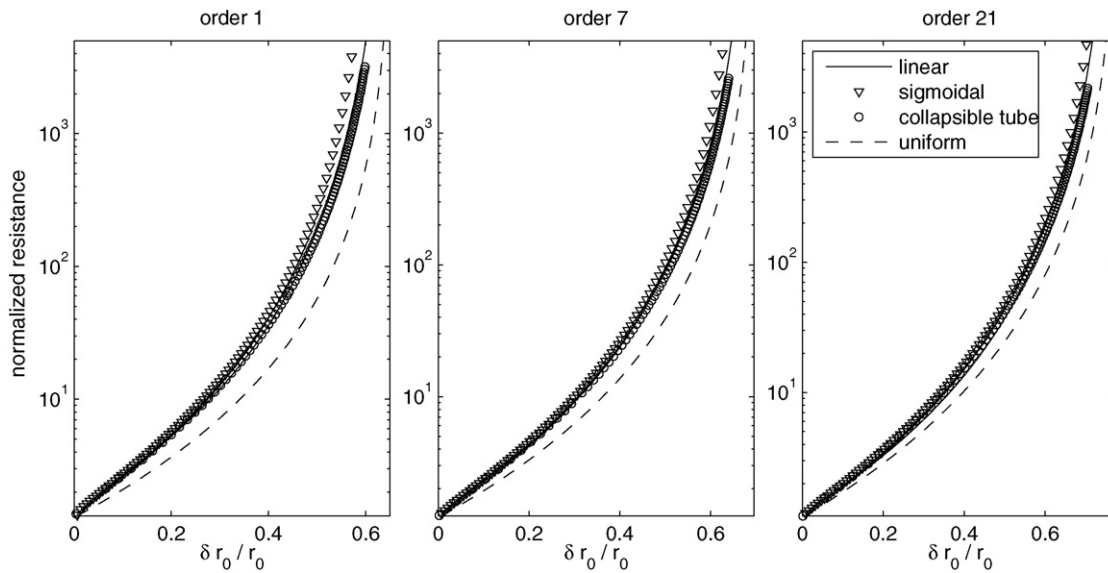


Fig. 5. Airway resistance increase due to folding. Normalised airway resistance as predicted by each folding model and uniform constriction for selected airway orders, as a function of normalised constriction. Resistance is normalised such that the value is 1 at $\delta r_0 = 0$. The increase in resistance is significant at even modest degrees of constriction, especially for the smaller orders. Normalised resistance is given on a log scale.

for all orders and all degrees of constriction. These error calculations are given in Fig. 7 both as an error boundary in the left panel and as an average error for each airway order in the right panel. Constriction is normalised such that at 0 the airway radius is r_0 and at 1 contact between folds occurs in the collapsible tube model.

The linear folding model compares very favourably with the collapsible tube model for all but very high degrees of constriction, though the relative error does not exceed 10% for any combination of airway order and degree of constriction. For all orders, the mean error between the two models is less than 3.1%. Because the largest errors occur near closure, the errors tend to be in resistance values that are already very high. As the airway resistance is so large as to be representing a nearly closed airway, the relative errors seen between the models are potentially less relevant to overall airflow results.

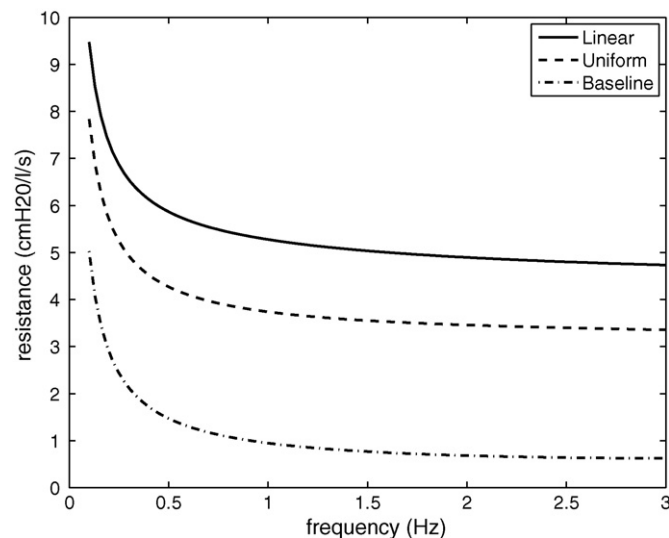


Fig. 6. Airway tree resistance. Total resistance is given for a sample airway tree containing 90 airways from Horsfield order 1 to 10. The dotted curve gives the baseline resistance with no constriction. The outer radius of each airway is then constricted by 20% and resistance calculated for both uniform constriction (dashed) and the linear folding model (solid).

4. Discussion

We have demonstrated a simplified model of airway narrowing due to mucosal folding in constricting airways. Under the assumptions of constant airway wall area and basement membrane perimeter during constriction, as well as liquid filling of the folded regions, we have demonstrated that this simplified model generates predictions of effective airway radius and corresponding airway resistance in good agreement with existing models.

We have assumed that each airway has a base level radius such that during dilation to larger radii, the basement membrane perimeter stretches, but during constriction to smaller radii, the basement membrane perimeter is constant. This assumption is in agreement with existing experimental evidence (McParland et al., 2004; Noble et al., 2005). A more sophisticated treatment of the perimeter of the basement membrane and epithelial length may have certain benefits; however, it is important not to compromise the analytic solution, which is critical to the value of this simplified model.

The need for a simplified model arises from the development of multiscale, spatially distributed models of the lung in which it is necessary to calculate airflow properties of many airways, for many degrees of constriction. The complexity of existing mucosal folding models in the literature prevents their use. Furthermore, in many models bronchoconstriction and airflow are coupled together in ways which critically determine the behaviour of the model (Anafi and Wilson, 2001; Venegas et al., 2005) but the contribution of mucosal folding to this relationship is not yet taken into account. The availability of a simplified model will allow the effects of folding to be easily taken into account in such models.

We have presented the simplified model in such a way that different assumed forms of the folded airway boundary may be used. However, the simplest version, the linear model, has proved to make predictions in best agreement with the existing collapsible tube model (Lambert and Wilson, 1972; Lambert et al., 1994). This is fortuitous, in that the linear model has a closed-form solution and does not involve solving an optimisation (or other computationally intensive) problem as with other folding models. The agreement between the linear model and the collapsible tube model is very good for all airways in this parameter set as demonstrated in Fig. 7.

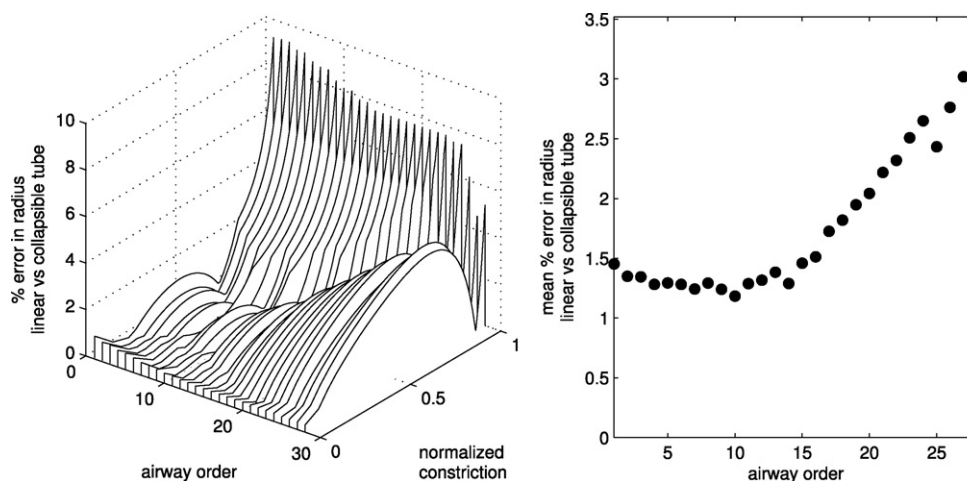


Fig. 7. Accuracy of linear model. Error in effective luminal radius predictions between the linear model and the collapsible tube model, for all airway orders and degrees of constriction. Left panel: 3D plot of error versus order and degree of constriction. The error at all points is less than 10%. Right panel: Mean error between the linear and collapsible tube model versus airway order, with mean error at all orders less than 3.1%.

There are many aspects of bronchial folding which have been considered important by authors in previous studies which we have neglected in this model including fluid–structure interaction (Heil, 1999; Heil and White, 2002; Heil et al., 2008), the role of folding and surface tension in determining the mechanical properties of the airway wall (Lambert and Wilson, 1972; Lambert, 1991; Lambert et al., 1994, 2001; Wiggs et al., 1992), mechanotransduction and the importance of compressive stresses (Tschumperlin et al., 2004; Tschumperlin and Drazen, 2006), and flow through the folded tube (without liquid filling of the folds) (Flaherty et al., 1972). For some applications it may be important to consider these factors. With this model we have only attempted to capture the geometrical aspects of airway narrowing rather than modifications to mechanical airway properties.

Models of airway pressure–radius relationships, particularly for peripheral airways, often rely on extrapolation from central airways (Lambert et al., 1982). Moreover, such models are expected to yield realistic airflow without any account of the possible effect of mucosal folding. A simplified model might be used to consider the contribution of mucosal folding to airway narrowing in such situations.

The assumptions made of a fixed, physiological number of folds for a given Horsfield order, as well as the assumption of symmetric folding patterns, are significant assumptions. The fixed number of folds arises as the best available choice among existing models, as previous attempts to determining the folding mode by minimising the associated strain energy have not demonstrated a high degree of accuracy. In part, this may be because of inaccuracies in what is known about the mechanical properties of the peripheral airways. In this work, we have made a fit to the best-available experimental data (Carroll et al., 2000; Okazawa et al., 1995) in order to determine the number of folds found in Table 1. Other experimental data sets, or a separate model, could alternately be used. However, while the number of folds is an important parameter, the results are not critically sensitive with respect to N —see Appendix B for a sensitivity analysis. Symmetric folding patterns are also a significant assumption; however, there is no obstacle to extending this type of analysis to accommodate, for example, self-similar folding patterns.

Likewise, assuming liquid filling of the folds (Yager et al., 1989) is an important assumption. In this study it provides an important simplification, allowing simple flow and resistance calculations within a cylindrical tube. The validity of the liquid-filling assumption is influenced by several factors: the number of folds; the severity of folding; the airway size. In particular, for large numbers of folds and relatively severe constriction, this assumption has

greater validity. Even if such deep, narrow folds are not entirely liquid-filled, the additional airflow allowed might be expected to be minimal. For smaller numbers of folds, incomplete liquid filling might have a greater influence on the airflow properties. The relatively large folding numbers (12–21) used in this study help to mitigate this deficiency; not only does the linear model provide better agreement with the collapsible tube model at these larger N values, but the liquid-filling assumption is stronger as well.

It may be possible to relax the liquid-filling assumption and explore the properties of flow through the deformed tube under various folding models (Flaherty et al., 1972). Even without liquid filling of the folds, folding may be expected to have a significant contribution to the airflow properties of the airway. However, under conditions of normal surfactant, the use of an airway wall model fit to experimental data, and the assumption of liquid filling of the folds, the model presented here provides an accurate and vastly simplified alternative.

Acknowledgement

This work was supported by NIH grant NHLBI R33HL87789.

Appendix A. Numerical solution of sigmoidal model

Under the sigmoidal form assumption, simple expressions for α and β are not available as Eq. (2) can only be evaluated as a Jacobi elliptic function. This is true of most assumed folding forms that one might try. However, the arclength integral can be integrated numerically and a simple optimisation performed to find the two parameters. Because the problem does not have multiple solutions and involves only two degrees of freedom, this still presents significantly less computational effort than required by the existing models.

Such a solution can easily be found using MATLAB by constructing a measure of the error

$$\epsilon(\alpha, \beta) = (A - A')^2 + (P - P')^2 \quad (\text{A.1})$$

where A and P are the initial wall area and membrane perimeter, respectively, A' is given by Eq. (5) and P' must be computed numerically. P' may be found by integrating Eq. (2) numerically using the MATLAB function `quad()`, which employs adaptive Simpson quadrature. Then Eq. (A.1) may be minimised for values of α and β using the MATLAB function `fminsearch()`, which uses a Nelder–Mead simplex optimisation method. Of course, other numerical methods may be employed. The approach described in

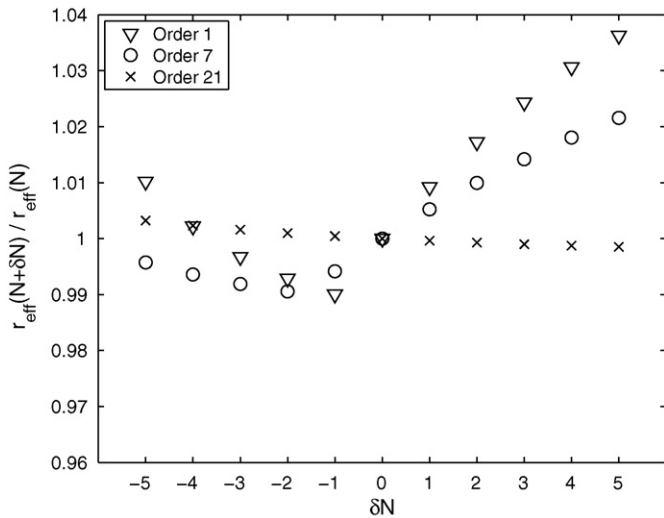


Fig. B.1. Sensitivity of r_{eff} to number of folds. For a selection of airway orders, we calculate the relative change in effective luminal radius under the linear folding model for folding numbers ranging from $N - 5$ to $N + 5$, where N is the experimentally determined folding number given in Table 1. Within the ± 5 fold range, there is no more than 4% change in the effective inner radius.

this appendix may also be used for other assumed folding forms for which no closed-form solution is available.

Appendix B. Sensitivity to number of folds

One concern about selecting *a priori* the number of folds is the sensitivity of the results to this parameter. To assess this sensitivity, we calculate the linear folding solution for $N - 5$ to $N + 5$ folds, where N is the folding number given in Table 1 as determined by the experimental data, under 20% constriction of r_0 . We take the offset in number of folds as $\delta N = (-5, \dots, 5)$ and measure $r_{\text{eff}}(N + \delta N)/r_{\text{eff}}(N)$ to assess the relative change in effective radius due to changes in the number of folds. The results of this analysis are given in Fig. B.1 for selected airways (Horsfield orders 1, 7 and 21). Within the ± 5 fold range, there is no more than 4% change in the effective inner radius.

References

Anafi, R.C., Wilson, T.A., 2001. Airway stability and heterogeneity in the constricted lung. *J. Appl. Physiol.* 91, 1185–1192. Carroll, N.G., Perry, S., Karkhanis, A., Harji,

- S., Butt, J., James, A.L., Green, F.H.Y., 2000. The airway longitudinal elastic fiber network and mucosal folding in patients with asthma. *Am. J. Respir. Crit. Care Med.* 161, 244–248.
- Flaherty, J.E., Keller, J.B., Rubinow, S.I., 1972. Post buckling behavior of elastic tubes and rings with opposite sides in contact. *SIAM J. Appl. Math.* 23, 446–455.
- Heil, M., 1999. Airway closure: Occluding liquid bridges in strongly buckled elastic tubes. *J. Biomech. Eng.* 121, 487–493.
- Heil, M., Hazel, A.L., Smith, J.A., 2008. The mechanics of airway closure. *Respir. Physiol. Neurobiol.* 163, 214–221.
- Heil, M., White, J.P., 2002. Airway closure: surface-tension-driven non-axisymmetric instabilities of liquid-lined elastic rings. *J. Fluid Mech.* 462, 79–109.
- Horsfield, K., Kemp, W., Phillips, S., 1982. An asymmetrical model of the airways of the dog lung. *J. Appl. Physiol.* 52, 21–26.
- Kamm, R.D., 1999. Airway wall mechanics. *Annu. Rev. Biomed. Eng.* 01, 47–72.
- Lambert, R.K., 1991. Role of bronchial basement membrane in airway collapse. *J. Appl. Physiol.* 71, 666–673.
- Lambert, R.K., Codd, S.L., Alley, M.R., Pack, R.J., 1994. Physical determinants of bronchial mucosal folding. *J. Appl. Physiol.* 77, 1206–1216.
- Lambert, R.K., Pare, P.D., Okazawa, M., 2001. Stiffness of peripheral airway folding membrane in rabbits. *J. Appl. Physiol.* 90, 2041–2047.
- Lambert, R.K., Wilson, T.A., 1972. Flow limitation in a collapsible tube. *J. Appl. Physiol.* 33, 150–153.
- Lambert, R.K., Wilson, T.A., Hyatt, R.E., Rodarte, J.R., 1982. A computational model for expiratory flow. *J. Appl. Physiol.* 52, 44–56.
- Lutchen, K.R., Gillis, H., 1997. Relationship between heterogeneous changes in airway morphometry and lung resistance and elastance. *J. Appl. Physiol.* 83, 1192–1201.
- Lynch, R.V., Ostberg, D.R., 1970. *Calculus*. Ginn-Blaisdell, Waltham, MA.
- McParland, B.E., Pare, P.D., Johnson, P.R.A., Armour, C.L., Black, J.L., 2004. Airway basement membrane perimeter in human airways is not a constant; potential implications for airway remodeling in asthma. *J. Appl. Physiol.* 97, 556–563.
- Noble, P.B., Sharma, A., McFawn, P.K., Mitchell, H.W., 2005. Elastic properties of the bronchial mucosa: epithelial unfolding and stretch in response to airway inflation. *J. Appl. Physiol.* 99, 2061–2066.
- Okazawa, M., Vedal, S., Verburgt, L., Lambert, R.K., Pare, P.D., 1995. Determinants of airway smooth muscle shortening in excised canine lobes. *J. Appl. Physiol.* 78, 608–614.
- Seow, C.Y., Wang, L., Pare, P.D., 2000. Airway narrowing and internal structural constraints. *J. Appl. Physiol.* 88, 527–533.
- Tschumperlin, D.J., Dai, G., Maly, I.V., Kikuchi, T., Laiho, L.H., McVittie, A.K., Haley, K.J., Lilly, C.M., So, P.T.C., Lauffenburger, D.A., Kamm, R.D., Drazen, J.M., 2004. Mechanotransduction through growth-factor shedding into the extracellular space. *Nature* 429, 83–86.
- Tschumperlin, D.J., Drazen, J.M., 2006. Chronic effects of mechanical force on airways. *Annu. Rev. Physiol.* 68, 563–583.
- Venegas, J.G., Winkler, T., Musch, G., Melo, M.F.V., Layfield, D., Tgavalekos, N., Fischman, A.J., Callahan, R.J., Bellani, G., Harris, R.S., 2005. Self-organized patchiness in asthma as a prelude to catastrophic shifts. *Nature* 434, 777–782.
- Wiggs, B.R., Bosken, C., Pare, P.D., James, A., Hogg, J.C., 1992. A model of airway narrowing in asthma and in chronic obstructive pulmonary disease. *Am. Rev. Resp. Dis.* 145, 1251–1258.
- Wiggs, B.R., Hrousis, C.A., Drazen, J.M., Kamm, R.D., 1997. On the mechanism of mucosal folding in normal and asthmatic airways. *J. Appl. Physiol.* 83, 1814–1821.
- Yager, D., Butler, J.P., Bastacky, J., Israel, E., Smith, G., Drazen, J.M., 1989. Amplification of airway constriction due to liquid filling of airway interstices. *J. Appl. Physiol.* 66, 2873–2884.